B1 Inhomogeneity Correction of In-vivo CEST Contrast

Anup Singh[1], Kejia Cai[1], Mohammad Haris[1], Hari Hariharan[1], and Ravinder Reddy[1]
[1]*Radiology, University of Pennsylvania, Philadelphia, Pennsylvania, United States*

INTRODUCTION: Chemical Exchange Saturation Transfer (CEST) MRI is being used for exploring metabolites/macromolecules with exchangeable protons which cannot be imaged using conventional MRI due to their low concentration (1-4). CEST contrast depends on solute exchange rate (k_{exs}), offset frequency ($\Delta\omega$), concentration, T_1 and T_2 values of water as well as the exchanging molecule, saturation pulse power amplitude (B_1) and duration. CEST contrast is highly sensitive to B_0 and B_1-inhomoginities and correction of these in-homogeneities is essential. Correction methods based upon steady state conditions are not suitable for in-homogeneities corrections of data in non-steady state conditions as used in current study. Recently, an elegant approach for B_0 homogeneities corrections is being adopted (5) in CEST literature which can be used for both steady and non-steady state conditions. Correction of CEST contrast for B_1-inhomgeneites is still challenging. At high field clinical/research scanners,B_1 in-homogeneities are present in substantial amount. In current study dependence of CEST contrast on saturation power is studied in human brain at 7T and a calibration based approach for B_1 field in-homogeneities correction is presented.

MATERIALS AND METHODS: In CEST experiments, the CEST effect of the solute spins is computed generally using following equation: $CEST_{asy}(\Delta\omega)=100*[M_{sat}(-\Delta\omega) - M_{sat}(+\Delta\omega)]/M_{sat}(-\Delta\omega)$ *[1]*, where M_{sat} ($\pm\Delta\omega$) are the water magnetization obtained with saturation at a '+' or '–' $\Delta\omega$ offset of the water resonance. The pulse sequence used in current study consists of a frequency selective saturation pulse train (SPT) (user selected saturation offset frequency ($\Delta\omega$), saturation duration and B_{1rms}) followed by a segmented RF spoiled GRE readout acquisition with centric phase encoding order. At the end of the acquisition, a variable delay has been added to provide T1 recovery. The SPT is composed of Hanning windowed rectangular pulses (99.8 ms pulse) and delays (0.2 ms) between them. The number of pulses in the train can be adjusted to provide variable saturation duration. The peak B_1 of the Hanning windowed pulse is set to provide the required B_{1rms} value.

***Human Studies*:** The study was conducted under an approved Institutional Review Board protocol of the University of Pennsylvania. Three subjects were taken from a normal population in the age range of 28-35 yrs. CEST imaging of the human brain were performed at 7T on a Siemens research scanner. The actual study protocol consisted of the following steps: a localizer, WASSR (5), z-spectral or CEST acquisitions and B_1 data collection. Z-spectral and CEST data on same volunteers were acquired on different day. For WASSR acquisitions, $\Delta\omega$ range of -1 to +1 ppm with step size of 0.05 ppm was used. For z-spectrum acquisitions, $\Delta\omega$ range of -6 to +6 ppm with step size of 0.5 ppm, $\Delta\omega$ range of ±7 to ±12 ppm with step size of 1 ppm, $\Delta\omega$ range of ±20 to ±60 ppm with step size of 10 ppm, and $\Delta\omega$ of ±100 ppm was used. In addition, base image without saturation (M_0) was also acquired. For CEST acquisitions, a limited $\Delta\omega$ range required for B_0 correction was used. Typical $\Delta\omega$ ranges used for CEST acquisitions were -2.5 to -3.5 ppm and 2.5 to 3.5 ppm with 0.25 ppm steps. For WASSR acquisitions, a 0.2 s SPT with B_{1rms} of 0.13 μT was used in all cases. For z-spectral data, a 1s SPT and multiple B_{1rms} of 0.7 μT, 1.4 μT, 2.2 μT, 2.9 μT were used. For investigating the effects of saturation parameters, multiple CEST images were collected at 7T using saturation pulses with B_{1rms} of 0.7 μT, 1.4 μT, 2.2 μT, 2.9 μT, 3.6 μT and 4.3 μT with duration of 1s. Data for generating B1 map was obtained using *flip and crush* pulse sequence with two flip angles (30 and 60 degree).

***Data analysis*:** B_0 map was computed using WASSR data (5) and used for correction of z-spectral data or CEST data (at ±3ppm) for B_0 in-homogeneities. Following B_0 in-homogeneities correction, z-spectral and asymmetry curves from multiple ROI's and CEST maps (at 3.0 ppm) were generated using Eq. [1]. B_1 map was computed using two flip angles data. Plots between CESTasy contrast and saturation powers were generated for different ROI's and polynomial of 2nd degree was fitted over a limited range of B_{1rms} for generating calibration parameters. CEST map at B_{1rms} of 2.9 μT corrected for B_1 in-homogeneities was generated using B_1 map and calibration parameters derived from GM/WM tissues.

RESULTS AND DISCUSSIONS: As shown in Fig.1, CEST asymmetry curve shows non-linear dependence on saturation power. Negative contrast at low value is due to the presence of magnetization exchange/ NOE effect (6) centered ~ -3ppm w.r.t. water and MT asymmetry. In asymmetry analysis this phenomenon is predominant at low B_1 and at high B_1 CEST effect (particularly from -NH2 (~1-4 ppm) and -OH (~0-2 ppm) protons) dominates it and contrast becomes positive. B_1 map from human brain at 7T is highly inhomogeneous (Fig 2) and due to this CEST contrast at 3 ppm without B_1 correction is difficult to interpret. Same problem exist for CEST maps at other offset frequencies. As such shape of CEST contrast vs B_{1rms} curves at 3ppm is quite complex, however, over the range of ~50% variations polynomial of 2nd degree can be fitted. Ideally for B_1 in-homogeneities correction one requires CEST data to be collected at multiple B_{1rms} (at least 3) so that CEST contrast at B_{1rms} of interest can be generated by using CEST contrast at multiple B_{1rms} data and B_1 map. However, this approach may not be clinically suitable due increase in scanning time. Calibration curve (fitted poly.) parameters were different in GM and WM tissues, however, both type of parameters resulted similar CEST map after B_1 correction. Moreover, calibration parameters derived from different volunteer also resulted in similar CEST map after correction. In conclusion, for normal volunteers' calibration parameters derived from GM and WM tissues resulted in similar B1-inhomogenity corrected CEST map, however, for pathological tissues these parameters may not work and need to generate separate calibration parameters.

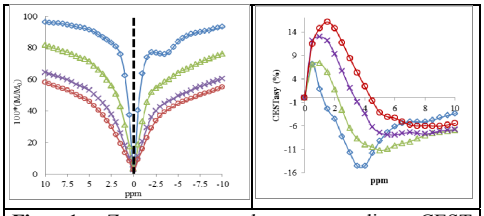

Fig. 1: Z-spectrum and corresponding CEST asymmetry curves for three saturation powers from gray matter area

REFERENCES: [1] Ward KM, et al., JMR 143, 79-87 (2000). [2]. Zhou J et al., Nat Med 9, 1085-1090 (2003). [3] Sun PZ, et al., MRM, 2007;58(6): 1207-15. [4] Kai K, et al., ISMRM 2011 (2781) [5] Kim M, et al., MRM, 2009;61(6):1441-50. [6] Narvainen J, et al., JMR 207 (2010) 242–250.

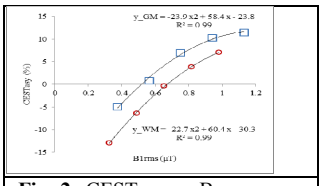

Fig. 2: CESTasy vs B_{1rms} curves from ROI in GM and WM brain tissues.

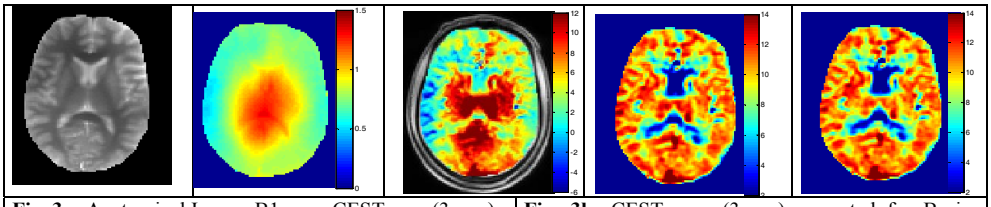

Fig. 3a: Anatomical Image, B1 map, CEST map (3ppm) without B1 inhomogeneity correction.

Fig. 3b: CEST map (3ppm) corrected for B_1 in-homogeneities using calibration parameters derived from WM and GM tissues respectively.

Acknowledgement: This study was funded by NCRR supported Biomedical Technology and Research Center